Mechanism of Thermal Efficiency Improvement in Twin Shaped Semi-Premixed Diesel Combustion

K. Inaba[1], Y. Zhang[1], Y. Kobashi[1], G. Shibata[1] and H. Ogawa[1]

[1]Hokkaido University, North 13, West 8, Kita-ku, Sapporo, 060-8628 Japan

Abstract

Improvements of the thermal efficiency in twin shaped semi-premixed diesel combustion mode with premixed combustion in the primary stage and spray diffusive combustion in the secondary stage with multi-stage fuel injection were investigated with experiments and 3D-CFD analysis. For a better understanding of the advantages of this combustion mode, the results were compared with conventional diesel combustion modes, mainly consisting of diffusive combustion. The semi-premixed mode has a higher thermal efficiency than the conventional mode at both the low and medium load conditions examined here. The heat release in the semi-premixed mode is more concentrated at the top dead center, resulting in a significant reduction in the exhaust loss. The increase in the cooling loss is suppressed to a level similar to the conventional mode. In the conventional mode the rate of heat release becomes more rapid and the combustion noise increases with advances in the combustion phase as the premixed combustion with pilot and pre injections and the diffusive combustion with the main combustion occurs simultaneously. In the semi-premixed mode, the premixed combustion with pilot and primary injections and the diffusive combustion with the secondary injection occurs separately in different phases, maintaining a gentler heat release with advances in the combustion phase. The mechanism of the cooling loss suppression with the semi-premixed mode at low load was investigated with 3D-CFD. In the semi-premixed mode, there is a reduction in the gas flow and quantity of the combustion gas near the piston wall due to the suppression of spray penetration and splitting of the injection, resulting in a smaller heat flux.

Keywords

Diesel engine, Thermal efficiency, Energy balance, Exhaust gas emissions, Heat release rate, Cooling loss, Multi-stage fuel injection, Premixed diesel combustion

Introduction

Premixed diesel combustion with a fuel injection relatively close to TDC, maintaining a sufficient ignition delay and ignition after the end of fuel injection with a large quantity of exhaust gas recirculation (EGR) has attracted much attention as a promising way for simultaneous reductions in nitrogen oxide (NOx) and particulate matter (PM) emissions as well as for achieving higher thermal efficiencies [1-10]. However, engine noise and limitations in the indicated mean effective pressure (IMEP) range due to the rapid combustion are serious issues impeding practical use. The rapid combustion can be suppressed with a large quantity of EGR, but carbon monoxide (CO) and total hydrocarbon (THC) emissions may increase with the increase in EGR, resulting in poorer thermal

efficiency [7]. To overcome these disadvantages, there are several reports of the semi-premixed diesel combustion mode, with a first-stage premixed combustion of the primary injection and a second-stage spray diffusive combustion of the secondary injection suppressing the rapid first-stage premixed combustion, realizing a wider IMEP range with overall milder combustion [11 - 22]. The CO and THC formed in the first-stage premixed combustion are oxidized with the second-stage spray combustion, resulting in the improvements in combustion efficiency. The authors have established efficient and clean semi-premixed diesel combustion mode with systematic investigations of the effects of operating parameters including intake gas and fuel injection conditions on the combustion characteristics over a wide operating range [18 - 20]. Optimizing the first-stage combustion fraction and the second injection timing to the position of the twin peak shape heat release, significant reductions in engine noise when compared with the premixed diesel combustion with a single injection were achieved, in addition to improved indicated thermal efficiency and decreased NOx emissions and without increases in other exhaust gas emissions, including the CO, THC, and smoke emissions [18]. A significantly high indicated thermal efficiency exceeding 50% is established with a reduction in the intake oxygen concentration due to the smaller cooling loss [19]. Both the heat flux value and the high heat flux area in the twin combustion are smaller than in the single premixed combustion due to decreases in the quantities of burned gas near the combustion chamber wall with the separated fuel injections, showing the mechanism of the reduction in cooling loss in the twin combustion [20].

In this report, the energy balances and the exhaust gas emissions in the optimized semi-premixed diesel combustion mode and in the typical conventional diffusive diesel combustion mode mainly with diffusive combustion were compared to show the superiority of the semi-premixed mode and the mechanisms of the thermal efficiency improvements were analysed with 3-D CFD analysis. The heat release of the semi-premixed mode can be more concentrated at the top dead center, expecting to realize a significant reduction in the exhaust loss and a higher thermal efficiency than the conventional diffusive diesel combustion mode.

Experimental Apparatus and Procedures

The experiments were conducted on a single cylinder, four-stroke cycle, supercharged, direct injection diesel engine with a common-rail fuel injection system and low pressure loop cooled EGR. The specifications of the engine are shown in Table 1. The stepped-lip re-entrant type combustion chamber shown in Figure 1 was used, establishing a reduction in cooling loss due to weaker in-cylinder gas motion with squish. A piezoelectric injector (Denso G3P) and ordinary diesel fuel (JIS No.2) were used in all experiments.

Table 2 shows the basic engine operating conditions. A low load (IMEP ≈ 0.4 MPa, 1500 rpm) and a medium load (IMEP ≈ 0.7 MPa, 2000 rpm) were examined in the semi-premixed and the conventional diffusive diesel combustion modes. The total fuel injection quantity, Q_{total} at each load is fixed and the indicated mean effective pressures of the two modes are slightly different due to the change in thermal efficiency. The intake gas pressures were set with a supercharger driven by an electric motor and the exhaust gas pressure was adjusted to be equal to the intake gas pressure with a throttle valve, which modelled turbo-charged operation. The cooled EGR was realized with the exhaust gas

passed through a diesel particulate filter (DPF) and an EGR cooler and the intake oxygen concentrations were set by adjusting the EGR quantity. The intake gas temperatures were set with an intercooler and a heater.

Table 1. Engine specifications

Engine type	DI, single cylinder
Bore and stroke	ϕ85 × 96.9 mm
Displacement	550 cm^3
Nozzle hole	0.104 mm × 10 - 156°
Compression ratio	16.3 : 1
Swirl ratio (ratio of swirl rpm to engine rpm)	1.6 : 1

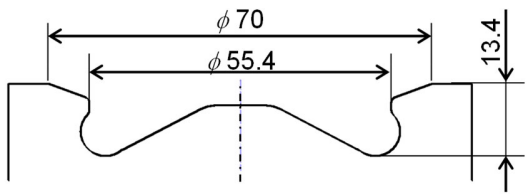

Figure 1. The stepped-lip re-entrant type combustion chamber.

Figure 2 shows the fuel injection patterns and the typical rates of heat release in the semi-premixed diesel combustion mode and in the reference conventional diffusive diesel combustion mode at a medium load with the same total injection quantity. In the semi-premixed mode, the three-stage fuel injection with the pilot, primary, and secondary injections shown in (a) was used and the ignition timings and combustion phases were optimized for the indicated thermal efficiency [20]. The conventional mode, shown in (b), mainly consists in diffusive combustion with three-stage fuel injection including the pilot, pre, and main injections. This conventional mode is authorized by all passenger car makers in Japan for reference and optimized in an engine for a commercial light duty vehicle with specifications similar to the engine in this experiment. In the conventional mode, relatively retarded combustion was applied to suppress the NOx emissions and the combustion noise with slight decreases in the thermal efficiencies. The quantity and timing at each fuel injection stage are shown in the bottom half of Table 2. In both combustion modes three stage fuel injection was applied, but the quantities at the first and the second (pilot and primary) injections in the semi-premixed mode are much larger than the pre and pilot injections in the conventional mode to increase the premixed combustion and to decrease the diffusive combustion. In the experiments to investigate the effect of the combustion phase, the injection timings at all stages were simultaneously varied from the timings shown in Table 2, maintaining the intervals and the quantities.

Table 2. Basic operating conditions

Engine load	Low		Medium	
Engine speed [rpm]	1500		2000	
Total fuel injection quantity, Q_{total} [mg/cycle]	10		18	
IMEP [MPa]	≈ 0.4		≈ 0.7	
Intake gas pressure, P_{in} [kPa]	102 (N.A.)		120	
Intake oxygen concentration, O_{2in} [%]	15.5		16.5	
Intake gas temp., T_{in} [˚C]	60		40	
Combustion mode	Semi-premixed	Conventional diffusive	Semi-premixed	Conventional diffusive
Pilot injection quantity [mg/cycle]	3	1.5	4.5	1.5
Primary (pre) injection quantity [mg/cycle]	3	1.5 (pre)	4.5	1.5 (pre)
Secondary (Main) injection. quantity [mg/cycle]	4	7 (Main)	9	15 (Main)
Pilot injection timing* [˚CA ATDC]	-13	-10	-10	-14
Primary (pre) injection Timing* [˚CA ATDC]	-7	-2.75	-2.5	-3
Secondary (Main) injection timing * [˚CA ATDC]	1.75	4	2.5	4.5
Fuel injection pressure [MPa]	100	100	200	135

* The injection timings at all stages were simultaneously varied, maintaining the intervals and the quantities in the investigation of the combustion phase effect.

The thermal efficiency related parameters were evaluated with the energy balance analysis. The energy balance during one cycle is described in Eq. (1).

$$\eta_i = \eta_u - \phi_{ex} - \phi_p - \phi_{other} \qquad (1)$$

η_i: The indicated thermal efficiency calculated with the fuel consumption per cycle and the in-cylinder pressure

η_u: The combustion efficiency calculated from the carbon monoxide (CO) and total hydrocarbon (THC) concentrations in the exhaust gas

ϕ_{ex}: The exhaust loss fraction calculated from the change in enthalpy between the exhaust and intake gases considering the change in the specific heat with the temperature and gas compositions

ϕ_p: The pumping loss fraction calculated with the in-cylinder pressure during the exhaust and intake strokes

ϕ_{other}: The other loss fractions, calculated from Eq. (1), including the cooling loss as the main component and also the unburned fuel diluted into the lubricant oil

The pumping loss in this experiment can be considered negligible as the exhaust gas pressure was adjusted to be equal to the intake gas pressure with a throttle valve. Further, as both fuel injection timings in the first and second stages are set to be not far from the TDC, the fuel diluted into the lubricant oil is negligible in this experiment and ϕ_{other} is considered to be the cooling loss, ϕ_w, which is finally calculated from Eq. (1) as $\phi_w = \eta_i - \eta_u - \phi_{ex}$.

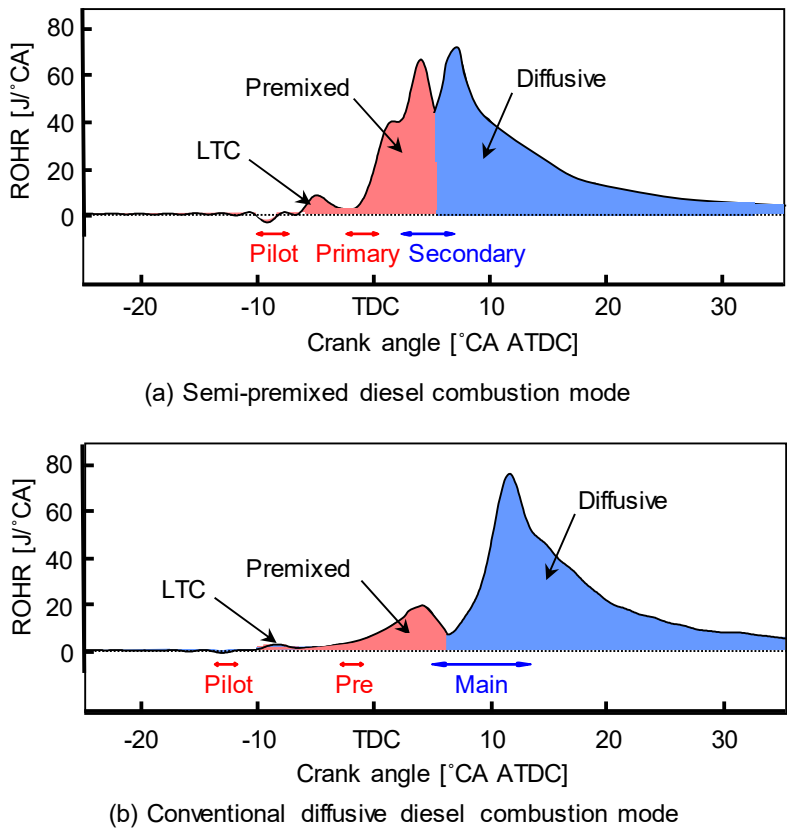

Figure 2. Fuel injection patterns and the typical rates of heat release in the semi-premixed combustion and the reference conventional diffusive diesel combustion modes at a medium load with the same total injection quantity (The red and blue arrows show the timing and durations of the fuel injections).

Computational Mesh and Sub-models in CFD analysis

To investigate the combustion characteristics of the semi-premixed diesel combustion mode and the conventional diffusive diesel mode, numerical simulations were conducted using the 3-D CFD code AVL FIRE v2014. 1. Figure 3 shows the computational mesh of the stepped-lip re-entrant combustion chamber. To reduce the calculation time, a 36° sector mesh (corresponding to a single nozzle hole of the ten holes) was adopted. The average cell size is 0.5 mm and the total number of cells is around 172,000. Table 3 shows the sub-models for the spray [23], the turbulence [24], the mixture formation [25], the chemical reaction [26], and the heat transfer [27]. The fuel injection rates measured with the Bosch

type rate of injection meter [28] in the experiments were applied for the simulations and the calculation was started from the IVC (intake valve closing).

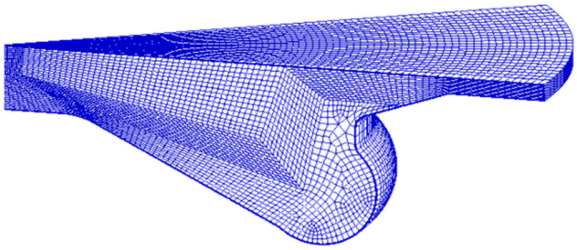

Figure 3. Computational mesh of the stepped-lip re-entrant combustion chamber release.

Table 3. Sub-models in CFD code FIRE

Spray	Discrete droplet model
Evaporation	Dukowitz[23]
Breakup	KH-RT[23]
Turbulence	*k-ζ-f* model[24]
Turbulence interaction	PDF-Hybrid[25]
Chemical reaction	Tsurushima[26]
Heat transfer model	Han-Reitz model[27]

Experimental Results and Discussion

Comparison between the Semi-Premixed Diesel Combustion mode and the Conventional Diffusive Diesel Combustion mode

Figure 4 shows the in-cylinder gas pressure and the rate of heat release (ROHR) from the semi-premixed diesel combustion mode and the conventional diffusive diesel combustion mode at the low and medium load conditions. Here, the arrows under the curves indicate the timings and durations at the pilot, primary, and secondary fuel injections for the semi-premixed mode and at the pilot, pre, and main injections for the conventional mode. The combustion phases of the semi-premixed mode are around the top dead center, more advanced than of the conventional mode at both load conditions here. In the semi-premixed modes at both the low and medium loads, the heat release with low temperature oxidation from the pilot injection can be clearly seen before the primary injection and the first stage premixed combustion starts just after the end of the primary (second) injection, showing typical HCCI combustion. Then, the second-stage diffusive combustion occurs just after the start of the secondary (third) injection. At the medium load, the two-stage premixed combustion with a shoulder shape just before the first peak due to the pilot and primary injections. The shoulder shaped part of the heat release is from the pilot injection and the first peak is mainly from the primary injection. The conventional modes at both loads also form two peaks; the first small peak is the premixed combustion from the pilot and pre injections and the second large peak is the diffusive combustion from the main injection. The quantities of the diffusive combustion of the semi-premixed modes are much

smaller than in the conventional modes at both load conditions. Higher load operation than the medium load (0.7 MPa IMEP) was attempted with the semi-premixed mode, but the quantity of the primary injection cannot be increased due to the excessively large rate of pressure rise and the advantages at low and medium loads decreased.

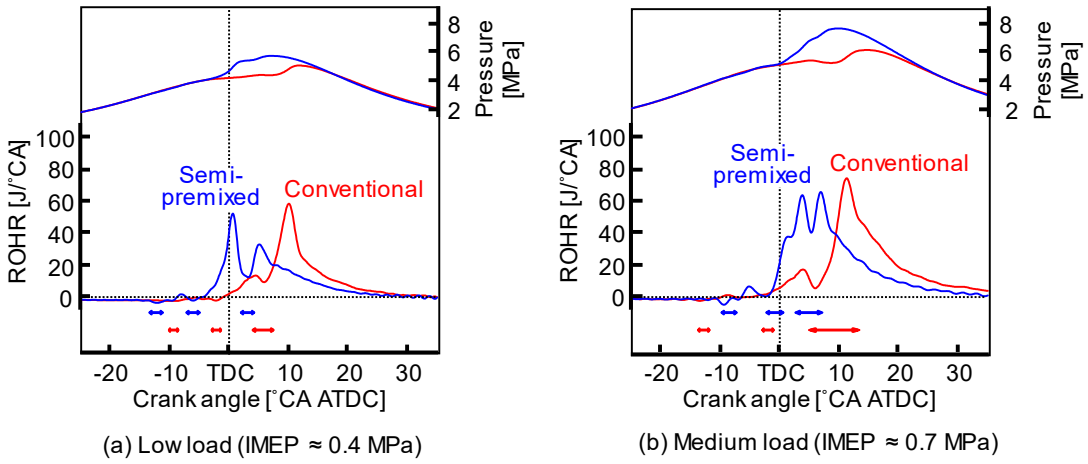

Figure 4. The in-cylinder gas pressure and the rate of heat release (ROHR) from the semi-premixed diesel combustion and the conventional diffusive diesel combustion

Figure 5 shows the energy balances at the same conditions as in Figure 4. The gross indicated thermal efficiencies, η_i in the semi-premixed diesel combustion modes are higher than in the conventional diffusive diesel combustion modes. This is due to smaller exhaust losses with the advances in the combustion phases. Especially, at the medium load, there is a 2.5% improvement in the indicated thermal efficiency with reductions in the exhaust loss without increases in the cooling loss. The cooling losses from the semi-premixed mode with the early combustion phases are similar to the conventional mode with the later combustion phases at the low and medium loads. The cooling loss generally displays a trade-off relation to the exhaust loss and increases with advances in the combustion phase. However, the increases in the cooling losses are suppressed in the semi-premixed combustion mode.

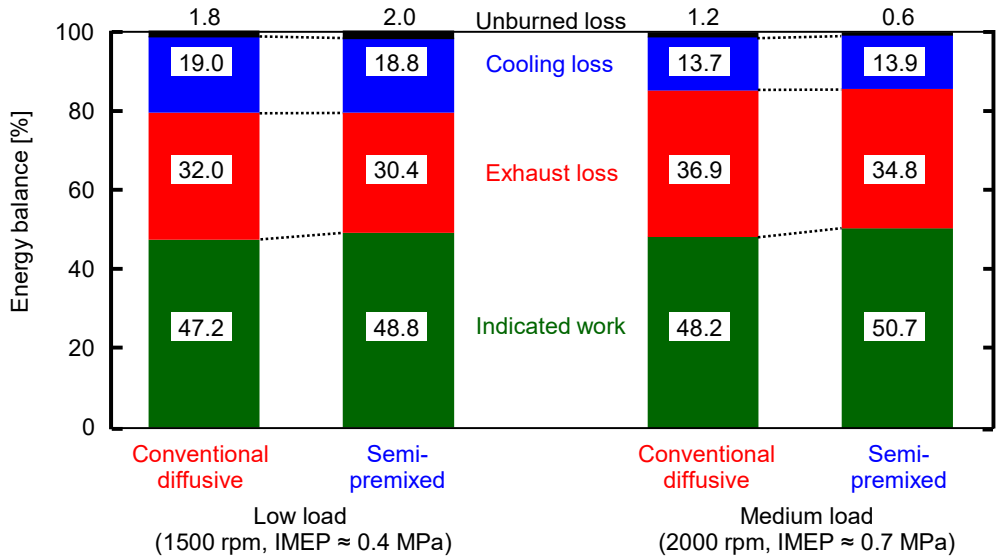

Figure 5. The energy balances at the same conditions as in Figure 4.

Figure 6 shows the maximum rate of pressure rise, $dP/d\theta_{max}$, the combustion noise, the NOx, and smoke emissions at the same conditions as in Figure 4. In the semi-premixed diesel combustion modes, the maximum rate of pressure rise and the combustion noise are larger at both loads due to the earlier combustion phases than in the conventional diffusive diesel combustion mode with the retarded combustion phases. However, the differences in combustion noise between the semi-premixed mode and the conventional mode are only 2 dBA at the low load and 1 dBA at the medium load, minimizing the increases in the combustion noise by the dividing of the combustion. At the medium load the smoke emissions in the semi-premixed mode are much lower than in the conventional mode, maintaining a similar low NOx level. At the low load the NOx and smoke emissions from the semi-premixed mode are sufficiently low, similar to the conventional mode.

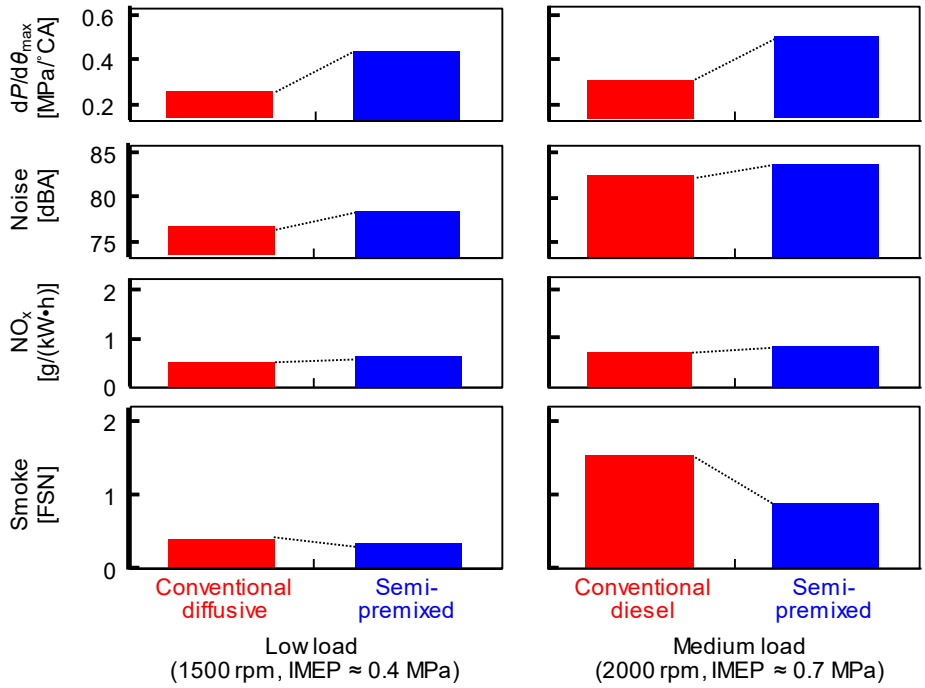

Figure 6. The maximum rate of pressure rise, $dP/d\theta_{max}$, the combustion noise, the NOx and smoke emissions at the same conditions as in Figure 4.

To summarize the results so far, the semi-premixed diesel combustion mode has the potential to improve the indicated thermal efficiency without increases in the combustion noise and exhaust gas emissions. However, in the conventional diffusive diesel combustion modes compared so far, the combustion phases are more retarded than the optimum for the thermal efficiency to suppress the NOx emissions and the combustion noise, and the indicated thermal efficiency can possibly be improved by advancing the combustion phases. To evaluate such an advantage of the semi-premixed mode the influence of the combustion phases on the characteristics in the semi-premixed and the conventional modes are compared and discussed in the next section.

Influence of the Combustion Phase

Figure 7 shows the in-cylinder gas pressure and the rate of heat release (ROHR) for different combustion phases changed with the fuel injection timings in the semi-premixed and the conventional diffusive diesel modes at the low load condition (IMEP ≈ 0.4 MPa). Here, the arrows below the diagrams indicate the fuel injection timings and the durations at each stage. In the conventional mode the rate of heat release becomes more rapid with advances in the combustion phase as the premixed combustion with pilot and pre injections and the diffusive combustion with the main combustion occurs simultaneously. In the semi-premixed mode, the shapes of the rate of heat release are not significantly changed and maintain the mild heat release like the premixed combustion with pilot and primary injections and the diffusive combustion with secondary injection occurs separately in the different phases.

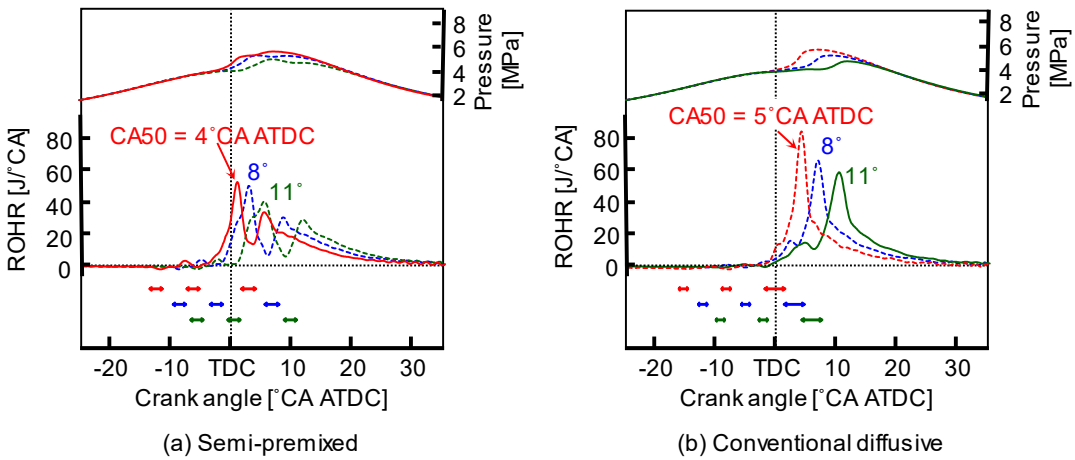

Figure 7. The in-cylinder gas pressure and the rate of heat release (ROHR) for different combustion phases (IMEP ≈ 0.4 MPa).

Figure 8 shows the influence of the combustion phase on the thermal efficiency related parameters (the indicated thermal efficiency, η_i, the combustion efficiency, η_u, the exhaust loss, ϕ_{ex}, and the cooling loss, ϕ_w) at the same conditions as in Figure 7, with the combustion phase (50% heat released crank angle, CA50) as in the abscissa. Here, the solid symbols (blue: semi-premixed, red: conventional) are the results also shown in Figure 4. As the combustion phase advances, the indicated thermal efficiencies improve, mainly due to decreases of the exhaust losses in both combustion modes. The exhaust losses in the semi-premixed mode are smaller than in the conventional mode at the same combustion phases, resulting in the higher indicated thermal efficiencies in the semi-premixed mode. The cooling loss in the conventional mode early in the combustion phase is larger than the other cases while there is no increase with advancing combustion phasing in the semi-premixed mode. The larger cooling loss in the early conventional mode may be due to the rapid combustion as suggested by Figure 7 (b), and a further reason for this will be discussed in 3.3 below.

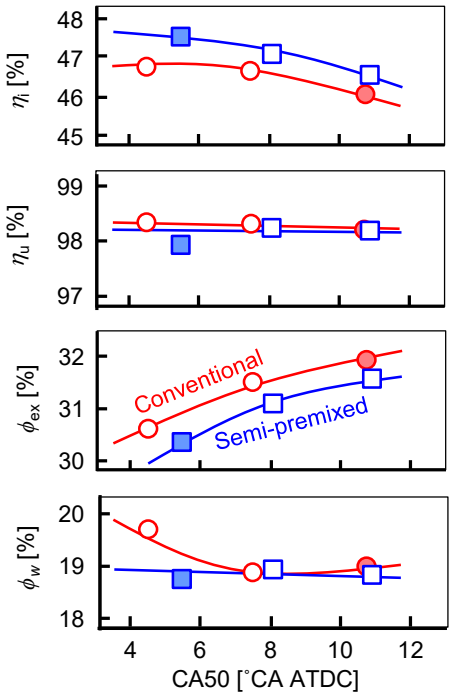

Figure 8. The influence of the combustion phase on the thermal efficiency related parameters (indicated thermal efficiency, η_i, combustion efficiency, η_u, exhaust loss, ϕ_{ex}, and cooling loss, ϕ_w) at a low load (1500 rpm, IMEP ≈ 0.4 MPa).

Figure 9 shows the NOx emissions, the maximum rate of pressure rise, $dP/d\theta_{max}$ and the combustion noise at the same conditions as in Figures 7 and 8. In both combustion modes the NOx emissions, the maximum rate of pressure rise, and the combustion noise increase as the combustion phases advance. Particularly, the NOx emissions and the combustion noise from the conventional combustion in the advanced CA50 condition are larger due to the rapid combustion shown in Figure 7.

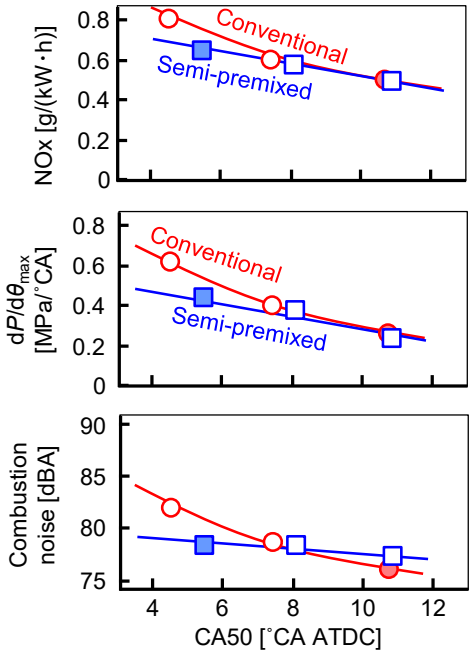

Figure 9. The NOx emissions, the maximum rate of pressure rise, $dP/d\theta_{max}$, the combustion noise, and the exhaust gas emissions at a low load (1500 rpm, IMEP ≈ 0.4 MPa).

Figure 10 shows the trade-off relation between the NOx and the indicated thermal efficiency with changing in the CA50. The indicated thermal efficiencies in the semi-premixed mode can be improved from the conventional diesel combustion mode when the NOx emissions are the same level.

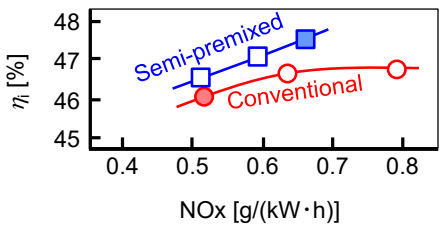

Figure 10. The trade-off relation between the NOx and the indicated thermal efficiency at a low load (1500 rpm, IMEP ≈ 0.4 MPa).

CFD Analysis on Mechanism of Thermal Efficiency Improvement in the Semi-premixed Diesel Combustion

As shown in Figure 8, when the combustion phases are advanced and optimized for the thermal efficiencies for both modes, the semi premixed combustion mode has higher thermal efficiency mainly due to the smaller cooling loss than the conventional diffusive mode. To elucidate the mechanism for this, the semi-premixed and conventional

combustion modes were analyzed with the 3-D CFD code (AVL FIRE), mainly focused on the cooling loss.

Figure 11 shows the semi-premixed and the conventional modes with (a) the experiments and (b) the CFD for the analysis of the mechanism of thermal efficiency improvement with the semi-premixed combustion mode. The analysis here is for the semi-premixed mode in the red solid curves in Figure 7 (a) and the conventional combustion in the red broken curves in Figure 7 (b), which show the early combustion phases and are optimized for the thermal efficiency in both modes. The results with the CFD are very similar to the experiments, assuring a sufficient validity of the CFD.

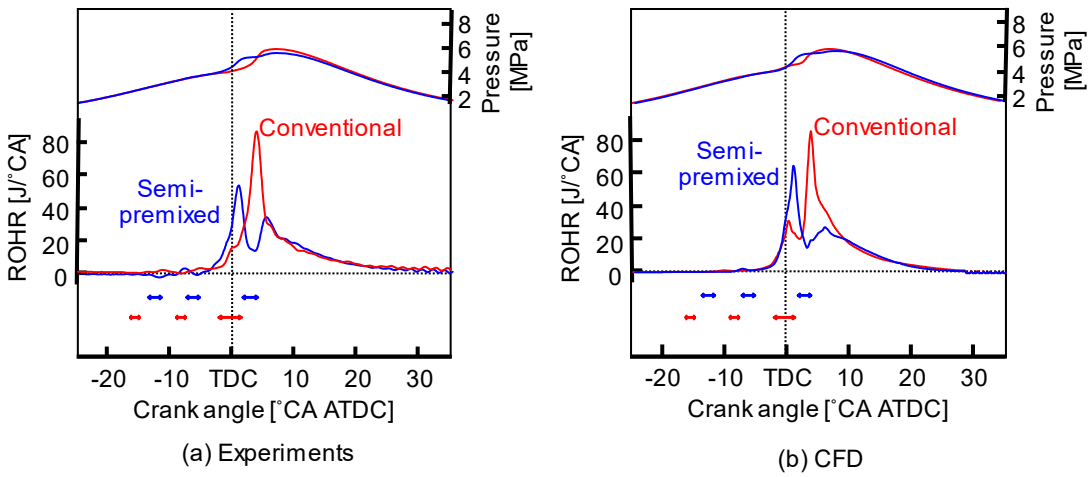

Figure 11. The semi-premixed and the conventional modes for the analysis on mechanism of thermal efficiency improvement with the semi-premixed mode (1500 rpm, IMEP ≈ 0.4 MPa).

Figure 12 shows the energy balances at the conditions in Figure 11. The results with the CFD are qualitatively similar to the experiments, showing the indicated thermal efficiency in the semi-premixed mode improves from the conventional diffusive mode mainly due to the reduction in the cooling loss.

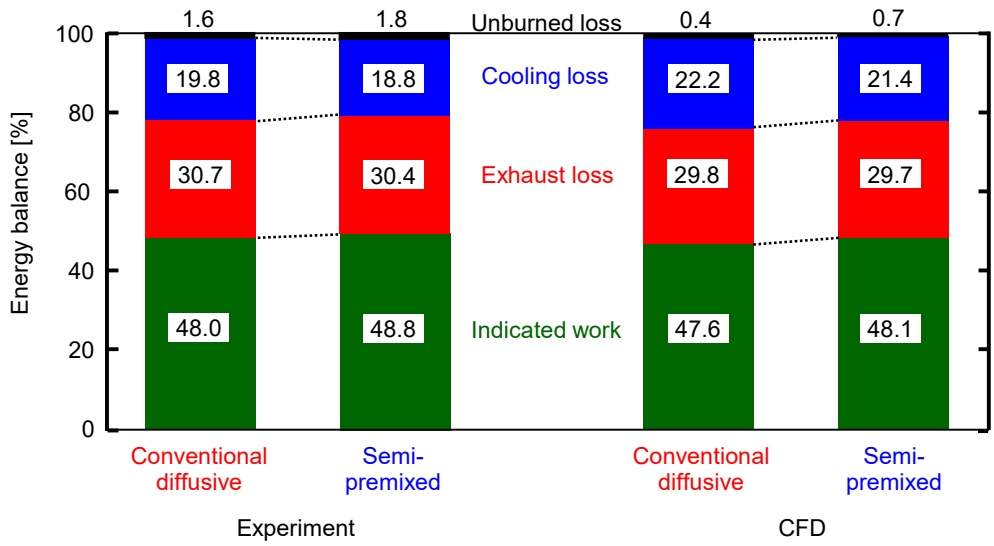

Figure 12. The energy balances at the conditions in Figure 11

Figure 13 shows the rate of cooling loss, $dQ_w/d\theta$ and the integrated cooling loss normalized by the total energy supply, Q_w with the CFD analysis (the in-cylinder pressure and the rate of heat release are shown in Figure 11 (b)). The percentages in the right panel show the calculated cooling loss differences from CA10 to CA50. In the conventional combustion mode, the rate of cooling loss rapidly increases just after the ignition and here the maximum rate of cooling loss is larger than in the semi-premixed combustion mode. The semi-premixed combustion mode shows the gentle increase of the rate of cooling loss with two stages and smaller $dQ_w/d\theta$, resulting in the much smaller cooling loss between CA10 and CA50.

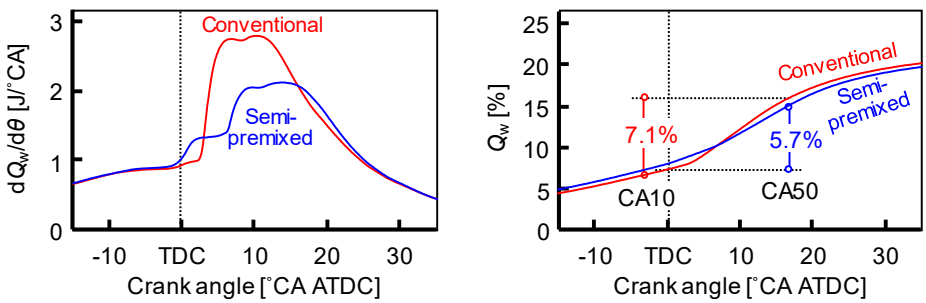

Figure 13. The rate of cooling loss, $dQ_w/d\theta$ and the integrated cooling loss normalized by the total energy supply, Q_w with the calculation (1500 rpm, IMEP ≈ 0.4 MPa).

Figure 14 shows the plots of gas temperature, gas velocity, and heat flux along the piston top surface shown in Figure 15. In the conventional mode at 4°CA ATDC the gas velocities are very fast and the high heat flux spreads widely on the lip of the combustion chamber where the fuel sprays impinge. In the semi-premixed combustion, there are also high temperature areas, but they are smaller and the gas velocities are much slower, resulting in the much smaller high heat flux areas despite the primary premixed combustion already having completed. This may be due to the slower impinging fuel spray on the piston wall and the decreases in the burned gas quantity near the piston wall due to the smaller fuel injection quantity per one stage and the suppression of fuel spray penetration with the dividing of the fuel injection. At 8°CA ATDC the high heat flux areas on the lip appears with the secondary combustion in the semi-premixed combustion, but the areas with high gas temperature, faster velocity, and high heat flux areas are smaller than in the conventional mode. At 12°CA ATDC the rates of heat release from both modes are similar as shown in Figure 11, but the high heat flux area in the semi-premixed mode is still smaller than in the conventional mode and the rate of cooling loss is much smaller as shown in Figure 13.

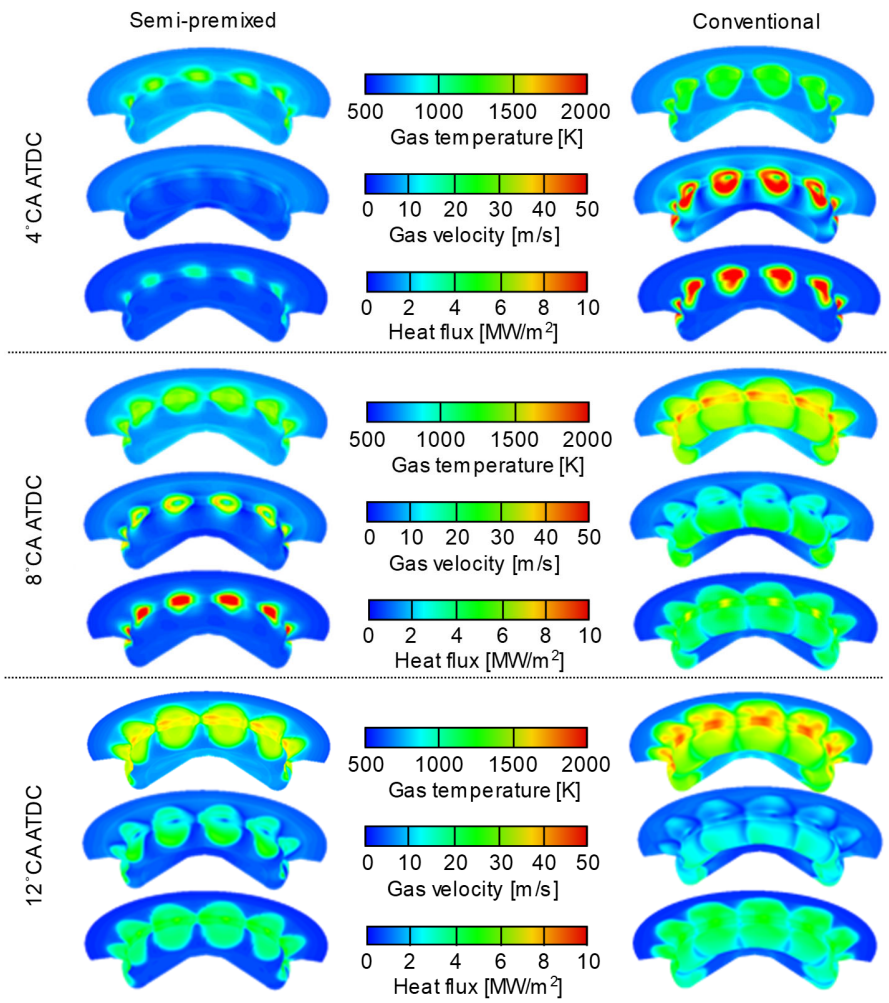

Figure 14. Plots of gas temperature, velocity, and heat flux along the piston top surface (1500 rpm, IMEP ≈ 0.4 MPa).

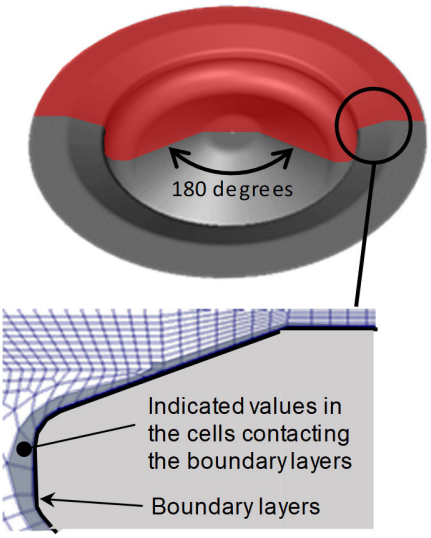

Figure 15. Indicated area of piston surface in Figure14.

Summary

In this paper, the twin shaped semi-premixed diesel combustion mode which releases half of the total heat with the premixed combustion and the conventional diesel combustion mode with mainly diffusive combustion were compared to show the superiority of the semi-premixed mode, and the mechanisms of the thermal efficiency improvements were analyzed with 3-D CFD analysis. The results may be summarized as follows:

1. The semi-premixed diesel combustion mode has a higher thermal efficiency than the conventional diffusive diesel combustion mode at both low and medium load conditions. The heat release of the semi-premixed mode is more concentrated at the top dead center, leading to significant reduction in the exhaust loss. In the semi-premixed combustion with the optimized combustion phase, the cooling losses are also smaller than the conventional mode with the similar combustion phasing.
2. In the semi-premixed diesel combustion mode, the maximum rate of pressure rise and the combustion noise is slightly larger at both the low and medium load conditions due to the earlier combustion phases than in the retarded conventional diffusive diesel combustion mode. However, the increases in combustion noise from the retarded conventional mode are only 2 dBA at the low load and 1 dBA at the medium load, the combustion noise minimized by dividing the combustion.
3. At the medium load the smoke emissions in the semi-premixed mode are much lower than in the retarded conventional mode without significant increases in NOx emissions. At the low load the NOx and smoke emissions from the semi-premixed mode are sufficiently low and similar to the retarded conventional mode.
4. In the conventional mode the rate of heat release becomes more rapid with advances in the combustion phase as the premixed combustion with pilot and pre injections and the diffusive combustion with the main combustion occurs simultaneously. In the semi-premixed mode, the premixed combustion with pilot and primary injections and the

diffusive combustion with secondary injection occur separately in the different phases, maintaining a gentle heat release with the advances in the combustion phase.

5. The CFD analysis showed that the cooling loss in the advanced conventional mode rapidly increases just after the ignition and that the maximum rates of cooling loss are much larger than in the semi-premixed combustion mode which shows a gentle increase with two stages, resulting in the much smaller cooling loss.
6. The range of high gas temperature and fast gas flows near the combustion chamber wall in the semi-premixed mode is smaller due to the smaller fuel injection quantity per injection stage when dividing the fuel injection than in the conditions of the advanced conventional mode, establishing the smaller heat flux and cooling loss.

Acknowledgements

This work was supported by the Council for Science, Technology and Innovation (CSTI), Cross-ministerial Strategic Innovation Promotion Program (SIP), "Innovative combustion technology" (funding agency: JST). The authors express their appreciation to Ms. Lucia del Bianco, a visiting student of Hokkaido University from Polytechnic University of Turin, for her cooperation in this research.

References

1. Akihama K, Takatori Y, Inagaki K, Sasaki S and Dean AM. Mechanism of the smokeless rich diesel combustion by reducing temperature. *SAE Technical Paper* 2001-01-0655, 2001.
2. Hasegawa R and Yanagihara H, HCCI combustion in DI diesel engine. *SAE Technical Paper* 2003-01-0745, 2003.
3. Ickes AM, Bohac SV and Assanis ND. Effect of fuel cetane number on a premixed diesel combustion mode. *Int. J. Engine Res* 2009; 10 (4): 251–263.
4. Li T, Izumi H, Shudo T, Ogawa H and Okabe Y. Characterization of low temperature diesel combustion with various dilution gases. *SAE Technical Paper* 2007-01-0126, 2007.
5. Li T, Suzuki M and Ogawa H, Effects of in-cylinder temperature and fuel air mixing quality on smokeless low temperature diesel combustion. *Proc. COMODIA 2008*, 2008; 135–142.
6. Li T, Suzuki M and Ogawa H. Characteristics of smokeless low temperature diesel combustion in various fuel–air mixing and expansion of operating load range. *SAE Technical Paper* 2009-01-1449, 2009.
7. Ogawa H, Li T and Miyamoto N. Characteristics of low temperature and low oxygen diesel combustion with ultra-high EGR. *Int. J. Engine Res* 2007; 8 (4): 365–378.
8. Takeda T, Nakagome K and Niimura K. Emission characteristics of premixed lean diesel combustion with extremely early staged fuel injection. SAE Technical Paper 961163, 1996.
9. Ogawa H, Xiong Q, Obe T, Sakane Y and Shibata G. Improvements in Thermal Efficiency of Premixed Diesel Combustion with Optimization of Combustion Related Parameters and Fuel Volatilities. *Int. J. Engine Res*; 2015: 16 (1): 81–91.
10. Krishnasamy A, Gupta SK and Reitz RD. Prospective fuels for diesel low temperature combustion engine applications: A critical review. *Int J Engine Res* 2020 (Online First).

11. Akagawa H, Miyamoto T, Harada A Sasaki S, Shimazaki N. Hashizume T and Tsujimura K. Approaches to Solve Problems of the Premixed Lean Diesel Combustion. *SAE Technical Paper* 1999-01-0183, 1999.
12. Hashizume T, Miyamoto T, Akagawa H et al. Combustion and emission characteristics of multiple stage diesel combustion. *SAE Technical Paper* 9821442, 1998.
13. Horibe N, Harada S, Ishiyama T and Shioji M. Improvement of premixed charge compression ignition based combustion by two-stage injection. *Int J Engine Res*; 2009: 10 (2): 71–80.
14. Kitamura T and Ito T. Mixing-controlled, low temperature diesel combustion with pressure modulated multiple-injection for HSDI diesel engine. *SAE Technical Paper* 2010-01-0609, 2010.
15. Kuzuyama H, Machida M, Kawae T, Tanaka T, Aoki, H, Sugiyama Y and Umehara T. High efficiency and clean diesel combustion concept using double premixed combustion: D-SPIA. SAE Technical Paper 2012-01-0906, 2012.
16. Fuyuto T, Taki M, Ueda R, Hattori Y, Kuzuyama H, and Umehara T. Noise and emissions reduction by second injection in diesel PCCI combustion with Split injection. *SAE Technical Paper* 2014-01-2676, 2014.
17. Ikeda, H, Iida N, Kuzuyama H, Umehara T, Fuyuto T. An investigation of controlling two-peak heat release rate for combustion noise reduction in split-injection PCCI engine using numerical calculation. *SAE Technical Paper* 2014-32-0132, 2014.
18. Ogawa H, Shibata G, Sakane Y and Obe T. Semi-premixed diesel combustion with twin peak shaped heat release using two-stage fuel injection. *SAE Technical Paper* 2016-01-0741, 2016.
19. Inaba K, Ojima Y, Masuko Y, Kobashi Y, Shibata G and Ogawa H. Thermal efficiency improvement with super-charging and cooled EGR in semi-premixed diesel combustion with a twin peak shaped heat release. *Int J Engine Res*; 2019: 20 (1), 80–91.
20. Inaba K, Masuko, Y, Zhang Y, Kobashi Y, Shibata G and Ogawa H. Thermal efficiency improvements with split primary fuel injections in semi-premixed diesel combustion with multi-peak shaped heat release. *SAE Technical Paper* 2019-01-2170, 2019.
21. Shibata, G, Ogawa H, Amanuma Y and Okamoto Y. Optimization of multiple heat releases in pre-mixed diesel engine combustion for high thermal efficiency and low combustion noise by a genetic-based algorithm method, *Int J Engine Res*; 2019: 20 (5), 540–554.
22. Molina, S, Antonio G, Monsalve-Serrano J and Villalta D. Effects of fuel injection parameters on premixed charge compression ignition combustion and emission characteristics in a medium-duty compression ignition diesel engine. *Int J Engine Res*; 2019 (Online First).
23. AVL FIRE VERSION 2014.1, Spray Module, 2014.
24. Hanjalic K, Popovac M and Hadziabdic M. A Robust Near-Wall Elliptic-Relaxation Eddy-Viscosity Turbulence Model for CFD. *Int J Heat and Fluid Flow*; 2004: 25(6): 1047-1051.
25. AVL FIRE VERSION 2017, General Gas Phase Reactions Module, 2017.
26. Tsurushima T. A new skeletal PRF kinetic model for HCCI combustion. *Proc Combust Inst*; 2009: 32(2): 2835–2841.
27. Han Z and Reitz RD. A temperature wall function formulation for variable density

turbulent flows with application to engine convective heat transfer modeling. Int J Heat and Mass Transfer; 1997: 40(3): 613-625.
28. Bosch W. The fuel rate indicator: A new measuring instrument for display of the characteristics of individual injection. SAE 660749, 1966.

Notation

CA50	*50% heat released crank angle*
EGR	*Exhaust gas recirculation*
IMEP	*Indicated mean effective pressure*
TDC	*Top dead canter*
η_i	*Indicated thermal efficiency*
η_u	*Combustion efficiency*
ϕ_{ex}	*Exhaust loss*
ϕ_p	*Pumping loss*
ϕ_{other}	*Other losses*
ϕ_w	*Cooling loss*